Revealing a 5,000-y-old beer recipe in China

Jiajing Wang[a,b,1], Li Liu[a,b], Terry Ball[c], Linjie Yu[d], Yuanqing Li[e], and Fulai Xing[f]

[a]Stanford Archaeology Center, Stanford University, Stanford, CA 94305; [b]Department of East Asian Languages and Cultures, Stanford University, Stanford, CA 94305; [c]Department of Ancient Scripture, Brigham Young University, Provo, UT 84602; [d]Zhejiang Research Institute of Chemical Industry, 310006 Hangzhou, China; [e]Department of Civil and Environmental Engineering, Stanford University, Stanford, CA 94305; and [f]Shaanxi Provincial Institute of Archaeology, 710054 Xi'an, China

Edited by Dolores R. Piperno, Smithsonian Institution, Fairfax, VA, and approved April 26, 2016 (received for review January 27, 2016)

The pottery vessels from the Mijiaya site reveal, to our knowledge, the first direct evidence of in situ beer making in China, based on the analyses of starch, phytolith, and chemical residues. Our data reveal a surprising beer recipe in which broomcorn millet (*Panicum miliaceum*), barley (*Hordeum vulgare*), Job's tears (*Coix lacryma-jobi*), and tubers were fermented together. The results indicate that people in China established advanced beer-brewing technology by using specialized tools and creating favorable fermentation conditions around 5,000 y ago. Our findings imply that early beer making may have motivated the initial translocation of barley from the Western Eurasia into the Central Plain of China before the crop became a part of agricultural subsistence in the region 3,000 y later.

Yangshao period | alcohol | starch analysis | phytolith analysis | archaeological chemistry

In China, the earliest written record of beer appears in oracle bone inscriptions from the late Shang dynasty (ca. 1250–1046 BC) (1, 2). According to the inscriptions, the Shang people used malted grains, including millets and barley/wheat (barley and wheat are represented by the same Chinese character, *lai*) as the main brewing ingredients (1, 3). Scholars have hypothesized that the Shang tradition of beer brewing has its origin in the Neolithic Yangshao period (5000–2900 BC), when large-scale agricultural villages were established in the Yellow River valley (4–6). The hypothesis is possible, considering that China has an early tradition of fermentation and evidence of rice-based fermented beverage has been found from the 9,000-y-old Jiahu site (7). Certain types of Yangshao vessels, including funnels and *jiandiping* (pointed-bottom vessel) amphorae, show stylistic similarities to the brewing equipment in the historical period and modern ethnographic records (6). However, direct evidence for alcohol production from Yangshao sites is lacking.

The Mijiaya site is located on a primary terrace northeast of the Chan River, a tributary of the Wei River, in Shaanxi, North China (Fig. 1 and *SI Text*). The excavations revealed two subterranean pits with artifacts that appeared to resemble in situ beer-brewing facilities (8) (Fig. 2 and Fig. S1). Both pits belong to Banpo IV (or late Yangshao period) stratum, and an established chronology based on ceramic typology and ^{14}C dates in the region securely places the time period between 3400 and 2900 BC (9, 10). Pit H82 was 3.7-m deep with straight walls and five steps leading down to the bottom (Fig. 2*A*); Pit H78 was 2.5–2.7 m deep with a flat bottom and a secondary platform on one side of the walls (8). Three types of vessels were recovered in both pits: wide-mouth pots, funnels, and *jiandiping* amphorae (Fig. 2 *B–D*), all of which have yellowish residues on their interior surface (Fig. S2). The shapes and styles of the vessels suggest three distinctive stages in the beer-making process: brewing, filtration, and storage. Interestingly, each pit also contained a pottery stove (Fig. 2*E*). In brewing activity, heating equipment is often used to maintain the optimal temperature for mashing. The stoves would have been especially suitable for this operation. Our hypothesis is that the artifact assemblages exclusively from the two pits represent a "beer-making toolkit." To test our hypothesis, we conducted starch, phytolith, and chemical analyses on the residues from two complete funnels and pottery sherds from five *jiandiping* amphorae and two wide-mouth pots.

Taxonomical Identification

The identification of starch grains and phytoliths was based on morphological and morphometric analyses. The morphological identification relied on a reference collection from over 1,000 Asian and European economically important plant specimens, and by consultation with published literature (11–16) (Table S1). For morphometric analysis, we applied two computer-assisted methods. First, a discriminant analysis model was used to separate the starch grains of Job's tears (*Coix lacryma-jobi*) from those of millets (*Setaria italica* and *Panicum miliaceum*). Based on three variables, including size, eccentricity of the hilum, and presence or absence of curved arms on the extinction cross, this multivariate model has a success rate of 82.4% for separating Job's tears from millets (17). Second, we conducted a morphometric analysis of the articulated dendritic phytoliths. Dendritics are produced in the inflorescence bracts of many common cereals, especially Triticeae species. Articulated dendritics produce wave patterns of taxonomic significance. Recent research has achieved good success at identifying wheat and barley phytoliths and distinguishing them from the relevant wild grasses (12, 13). A sample size as small as 30 dendritic wave lobes can be adequate for a 90% confidence level in discriminating among taxa based on differences in several wave lobe-shaped morphometries. We measured the wave lobes of articulated dendritic phytoliths from six Mijiaya residue samples following the procedures outlined by Ball et al. (18). Each residue sample yielded at least 30 measurable wave lobes in total, which allowed us to have statistical confidence in the measurements of form factor, roundness, convexity, solidity, compactness, and aspect ratio (Table S2). We compared the means of these six morphometries for the Mijiaya dendritics from each sample with the range of means observed in 20 Triticeae and other dendritic-producing species, including common

Significance

This research reveals a 5,000-y-old beer recipe in which broomcorn millet, barley, Job's tears, and tubers were fermented together. To our knowledge, our data provide the earliest direct evidence of in situ beer production in China, showing that an advanced beer-brewing technique was established around 5,000 y ago. For the first time, to our knowledge, we are able to identify the presence of barley in archaeological materials from China by applying a recently developed method based on phytolith morphometrics, predating macrobotanical remains of barley by 1,000 y. Our method successfully distinguishes the phytoliths of barley from those of its relative species in China.

Author contributions: J.W. and L.L. designed research; J.W., L.L., T.B., and F.X. performed research; J.W., L.L., T.B., L.Y., and Y.L. analyzed data; and J.W., L.L., and T.B. wrote the paper.

The authors declare no conflict of interest.

This article is a PNAS Direct Submission.

[1]To whom correspondence should be addressed. Email: jiajingw@stanford.edu.

This article contains supporting information online at www.pnas.org/lookup/suppl/doi:10.1073/pnas.1601465113/-/DCSupplemental.

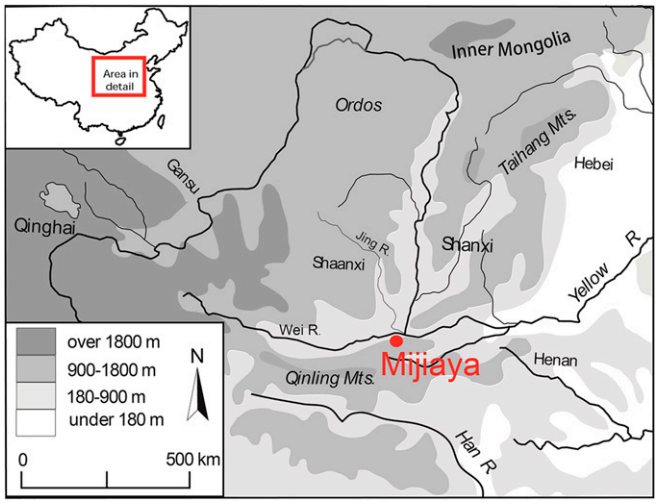

Fig. 1. Geographical Location of the Mijiaya Site.

wild species indigenous to China and domesticated species introduced into China from Western Eurasia (Tables S3 and S4).

Results

A total of 541 starch grains were recovered from the funnels and pottery sherds (Table 1). Of these grains, 488 starch grains (90.2% of the total) were identifiable to various taxonomic levels compared with our reference data. The starch assemblage mainly consists of millet, Triticeae, and Job's tears, with a smaller contribution from tubers that include snake gourd root (*Trichosanthes kirilowii*), yam (*Dioscorea* sp.), and lily (*Lilium* sp.) (Fig. 3 *A*–*F*). A high percentage of starch grains (n = 166, 30.7%) exhibit signs of damage, and among them two types of damage closely resemble that produced by beer brewing. First, some grains show pits and channels on their surface, ranging from being slightly pitted to completely hollow (Fig. 4*A*). Second, a large number of starch grains are swollen, folded, and distorted (Fig. 4*B*); some still retain their individual boundaries, but many merge into one another. These two damage patterns precisely match the morphological changes developed during malting and mashing, as we observed in our brewing experiments and that reported in published literature (Fig. 4 *C* and *D*, Fig. S3, and *SI Materials and Methods*) (19–22). During malting, enzymes in sprouting cereals break down starch to dextrins and simple sugars, creating typical surface pits and interior channels in the grains (19). Furthermore, mashing involves heating of the malt in water for a period, which causes gelatinization, swelling, folding, and distortion of starch grains (19). Thus, the damaged state of the starch grains in our archeological sample provides strong evidence for the conclusion that those starch grains are residues from the brewing process.

Phytolith data indicate the presence of cereal husks (Table 2). Phytoliths identified to the Panicoideae grass subfamily predominate the assemblage. Seven vessels revealed η-shaped long cells that are consistent with phytoliths formed in epidermal husk tissues of broomcorn millet (Fig. 3*J*) (15). Cross-shaped phytoliths showing a considerable variation in form and size, comparable with the crosses produced by Job's tears in our modern references, were observed (Fig. 3*H*). Phytolith forms produced in Pooideae were also identified. In particular, articulated dendritic phytoliths consistent in pattern and shape with those produced in the husks of Triticeae species were observed (Fig. 3*K*). Our morphometric analysis of the articulated dendritics indicates their most probable origin to be from the inflorescence bracts of barley (*Hordeum vulgare*). Although some of the mean measurements of the archaeological samples fall within the ranges of other taxa, all of the means fall within those observed in *H. vulgare* (Tables S5 and S6). The profile of phytoliths corroborates the starch grain assemblage, indicating the presence of broomcorn millet, Job's tears, and barley.

Our ion chromatographic (IC) analysis identified the presence of oxalate, which develops during the steeping, mashing, and fermentation of cereals (23). Calcium oxalate is a principle component of "beerstone," which settles out at the beer fermentation and storage containers, and has been used as a compound marker for identifying barley beer fermentation in ancient vessels (24–27). We conducted tests on the residues from Funnel 1, Pot 3, and Pot 5. The results confirmed that high levels of oxalate are present in Funnel 1 and Pot 5 (Fig. 5). Oxalate was not detected from Pot 3. The oxalate concentration is 0.08% (80 mg/100 g) for Funnel 1 and 0.05% (50 mg/100 g) for Pot 5. Although oxalates occur naturally in plants like spinach (*Spinacia oleracea*), rhubarb (*Rheum rhabarbarum*), and some *Dioscorea* and *Lilium* species, the vessel types in this study are not suitable for storing any fresh plant.

To rule out the potential contamination from the enclosing soil matrix and postexcavation conditions, we analyzed four samples as control specimens. Three samples were analyzed for starch and phytolith, including one from the sediment adhering to the exterior surface of Pot 5 (control sample 1), one from a stone adze fragment recovered from Pit H78 (control sample 2), and one from the plaster material used for reconstructing Funnel 2 (control sample 3) (Fig. S1). Compared with ancient samples, the control samples contained a much smaller number of phytoliths and starch grains (Tables 1 and 2) with no signs of damage. IC analysis of the exterior scrapings from Pot 5 (control sample 4) detected no oxalate, a result in clear contrast to a high level of oxalate found in the interior surface of the same vessel. These observations suggest that the high concentrations of starch, phytolith, and chemical residues related to the beer-making process are exclusively present on the interior surfaces of the Mijiaya vessels, which potentially have had direct association with beer brewing.

Discussion and Conclusion

All three lines of evidence are consistent with the archaeological data, indicating that the Yangshao people brewed a mixed beer with specialized tools and knowledge of temperature control. Our data show that the Yangshao people developed a complicated fermentation method by malting and mashing different starchy plants. Compared with millets, barley has much higher α- and β-amylase activities, which promotes the saccharification process (28). Tubers

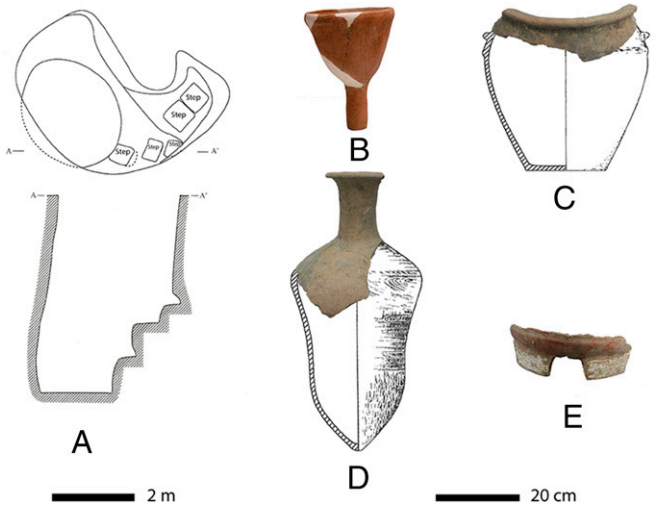

Fig. 2. The "beer-making toolkit" from Mijiaya Pit H82: (*A*) Pit H82 illustration in top and cross-section views, (*B*) funnel 1, (*C*) pot 6 in reconstructed form, (*D*) pot 3 in reconstructed form, and (*E*) pottery stove.

Table 1. Counts of starch grain types from vessels

Artifact no.	Triticeae	Job's tears, *C. lacryma-jobi*	Millet, *P. miliaceum*	Snake gourd root, *T. kirilowii*	Lily, *Lilium* sp.	Yam, *Dioscorea* sp.	Tuber*	UNID	Total	Damaged
Funnel 1	24	49	78	0	0	0	0	7	158	47
Funnel 2	23	13	11	4	0	1	2	4	58	19
Pot 1	17	6	3	1	0	0	10	3	40	6
Pot 2	7	3	3	0	0	1	0	1	15	14
Pot 3	11	5	11	0	0	0	1	9	38	23
Pot 4	39	17	23	2	3	1	6	6	98	20
Pot 5	11	19	14	9	0	0	7	4	66	17
Pot 6	14	10	7	0	1	0	4	14	50	15
Pot 7	6	6	4	0	0	0	1	5	24	5
Total	152	128	154	16	4	3	31	53	541	166
Percent, %	28.61	23.7	28.5	3.0	0.7	0.6	5.7	9.8	100.0	30.7
Control sample 1	1	0	0	0	0	0	0	2	3	0
Control sample 2	3	0	0	0	0	0	0	3	6	0
Control sample 3	0	0	0	0	0	0	1	3	4	0

*A general category that includes snake gourd root, lily, and yam. UNID, unidentified.

contribute starch and sugars for fermentation, and they also add a sweeter flavor to the beer. The Yangshao people probably developed their recipe through repeated experiments.

The discovery of barley in the beer residues suggests a social motivation in the initial stage of crop translocation (29). Barley was first domesticated in Western Eurasia and later introduced into China, presumably through the Central Asian steppe. The timing and nature of the crop's initial adoption in China is still not well understood (29–31). In the Central Plain, macrobotanical remains from the Yangshao sites are generally well preserved, dominated by millets and very few other cereal types, and no evidence of barley has been reported. The earliest evidence of barley comes from some sporadic finds in Bronze Age sites, all dated around or after 2000 BC (31, 32). Not until the Han dynasty (206 BC–AD 220), three millennia after Mijiaya, had this crop become an important part of

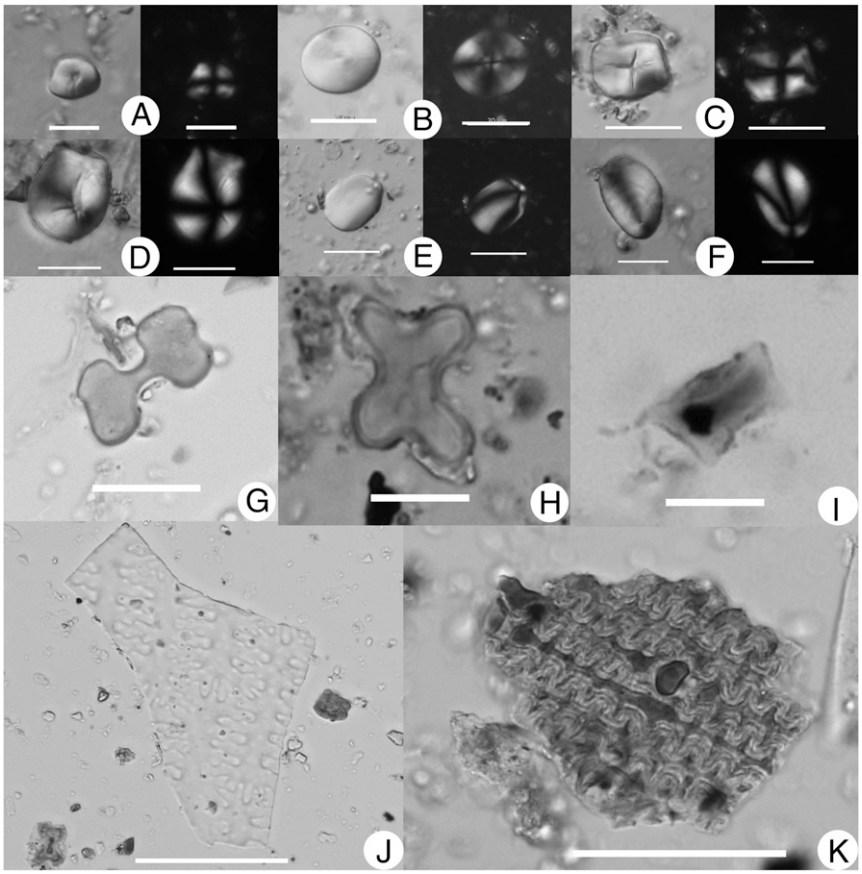

Fig. 3. Starch and phytolith types from Mijiaya vessels (the starch types showing DIC and polarized views): (*A*) Broomcorn millet (*P. miliaceum*). (*B*) Triticeae. (*C*) Job's tears (*C. lacryma-jobi*). (*D*) Snake gourd root (*T. kirilowii*). (*E*) Yam (*Dioscorea* sp.). (*F*) Lily (*Lilium* sp.). (*G*) Bilobate. (*H*) Cross. (*I*) Rondel. (*J*) η-shaped phytoliths, consistent with broomcorn millet. (*K*) Dendritic epidermal phytoliths, consistent with barley (*H. vulgare*). (Scale bars: 10 μm in *A*, *H*, and *I*; 20 μm In *B*–*G*; 50 μm in *J* and *K*.)

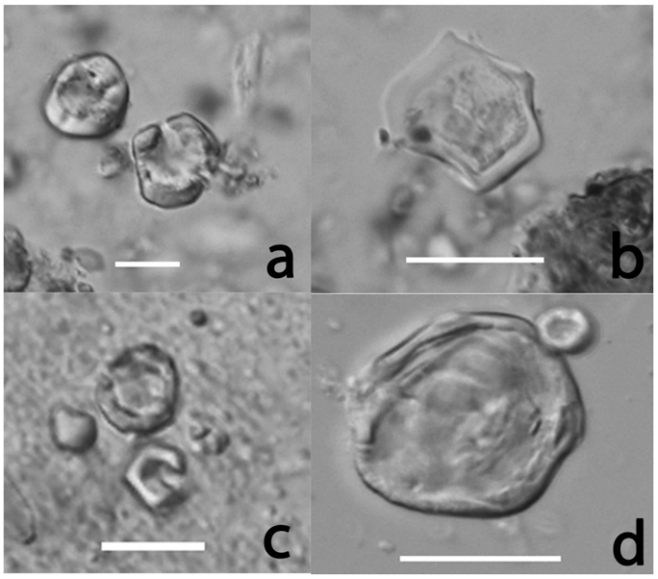

Fig. 4. Damaged starch grains from Mijiaya vessels and brewing experiments. (*A*) Mijiaya starch grains showing pitting and channeling. (*B*) A Mijiaya starch grain showing swollen, folded, and distorted characteristics. (*C*) Fermented broomcorn millet (*P. miliaceum*) starch grains from the brewing experiment using broomcorn millet and barley (*H. vulgare*). (*D*) A fermented gelatinized starch grain from the brewing experiment using broomcorn millet and barley. (Scale bars: 10 μm in *A* and *C*; 20 μm in *B* and *D*.)

subsistence in the Central Plain (29, 33). The microbotanical remains of barley at Mijiaya account for the earliest occurrence of this crop in China.

It is possible that the few rare finds of barley in the Central Plain during the Bronze Age indicate their earlier introduction as rare, exotic food. The Mijiaya farmers probably obtained small quantities of barley grains through exchange or cultivated the plant along with other cereals. We suggest that barley was initially introduced to the Central Plain as an ingredient for alcohol production rather than for subsistence. Because to our knowledge this is the first study that applies morphometric analysis to the dendritic phytoliths from China, future research with more comprehensive phytolith data from other Neolithic contexts is needed to test our hypothesis.

The practice of beer brewing is likely to have been associated with the increased social complexity in the Central Plain during the fourth millennium BC The late Yangshao period in the Wei River region was characterized by hierarchically organized settlement patterns, interpolity competitions, construction of large public architectures at regional centers, and ritual feasting likely organized by elite individuals and involving alcohol consumption (34) (*SI Text*). Like other alcoholic beverages, beer is one of the most widely used and versatile drugs in the world (35), and it has been used for negotiating different kinds of social relationships. The coincidence of beer production with other lines of material evidence suggests that competitive feasting was actively developing. The production and consumption of Yangshao beer may have contributed to the emergence of hierarchical societies in the Central Plain, the region known as "the cradle of Chinese civilization."

Materials and Methods

Residue Extraction Methods Summary. Chemical samples and two control samples (1, 3) were obtained by scraping off the sediments from the pottery surfaces with clean blades. Other residue samples were extracted by using an ultrasound bath or an ultrasound toothbrush. Starch and phytolith samples were floated from the residues using the heavy liquid sodium polytungstate at a specific gravity of 2.35. Extractions obtained from the residue samples were mounted in 50% (vol/vol) glycerol and 50% (vol/vol) distilled water on glass slides and scanned under a Zeiss Axio Scope A1 fitted with polarizing filters and differential interference contrast (DIC) optics, at 200× and 400× for both starches and phytoliths. Images were taken using a Zeiss Axiocam Hrc3 digital camera and Zeiss Axiovision software v4.8. See *SI Materials and Methods* for details.

Determination of Oxalate Using IC. Residue samples from Funnel 1, Pot 3, and Pot 5 were analyzed by a Dionex ICS 5000 with a conductivity detector, in Zhejiang Research Institute of Chemical Industry. The columns used were an Ion Pac-AS 11-HC Analytical (250 × 4 mm I.D.) and an Ion Pac AG11-HC guard column (40 × 4 mm I.D.) with an anion ASRS suppressor, operated at 20 °C. The eluent was 20 mM KOH and the flow rate was 1.5 mL/min; the injection loop was 25 μL. Each residue sample produced two experimental samples. Each experimental sample (0.03 g) was dissolved in 3 mL nitric acid and diluted with 50 mL distilled water. Standard solutions were made from solutions of sodium oxalate in a concentration range between 0.0005 and 0.002 mg/mL. The calibration curve was established by linear regression analysis of peak height vs. added concentration of oxalate. The detection limit for oxalate under the given conditions is 0.036%. Control sample 4 was analyzed by a Dionex DX-500 IC with a conductivity detector, in the Environmental Measurements Facility at Stanford University. The eluent was 20 mM NAOH and the flow rate was 1 mL/min. Standardized solutions were made from solutions of oxalic acid in a concentration range between 0.1 and 10 mg/mL. Other laboratory conditions were the same as those used for the three residue samples.

ACKNOWLEDGMENTS. We thank Dr. Maureece Levin, Mike Bonomo, and David Hazard for their comments on previous drafts of the paper; Dr. Zhouyong Sun for making arrangement and providing access to the data;

Table 2. Counts of phytolith types from vessels

Phytolith types	Taxonomic association	Funnel 1	Funnel 2	Pot 1	Pot 2	Pot 3	Pot 4	Pot 5	Pot 6	Pot 7	Total	Control sample 1	Control sample 2	Control sample 3
η-Type epidermal sheet element	(*P. miliaceum*)	4	3	0	3	1	3	5	0	6	25	2	0	0
Cross	(*Panicoideae*)	37	23	26	81	32	63	52	45	35	394	0	2	0
Bilobate	(*Panicoideae*)	49	18	16	62	26	24	50	22	15	282	0	2	0
Polylobate	(*Panicoideae*)	3	2	2	14	2	14	1	5	1	44	0	1	0
Articulated dendritic	(*Triticeae*)	2	11	0	76	33	24	27	4	0	177	0	0	0
Undulate trapezoid	(*Pooid*eae)	4	4	0	2	7	4	3	3	0	27	0	0	0
Epidermal sheet element	(*Poaceae*)	0	14	4	12	12	12	11	6	11	82	4	0	3
Bulliform	(*Poaceae*)	4	3	5	0	1	3	2	3	0	21	0	0	0
Rondel	(*Poaceae*)	14	2	4	4	2	4	6	1	3	40	0	1	0
Total		117	80	57	254	116	151	157	89	71	1,092	6	6	3

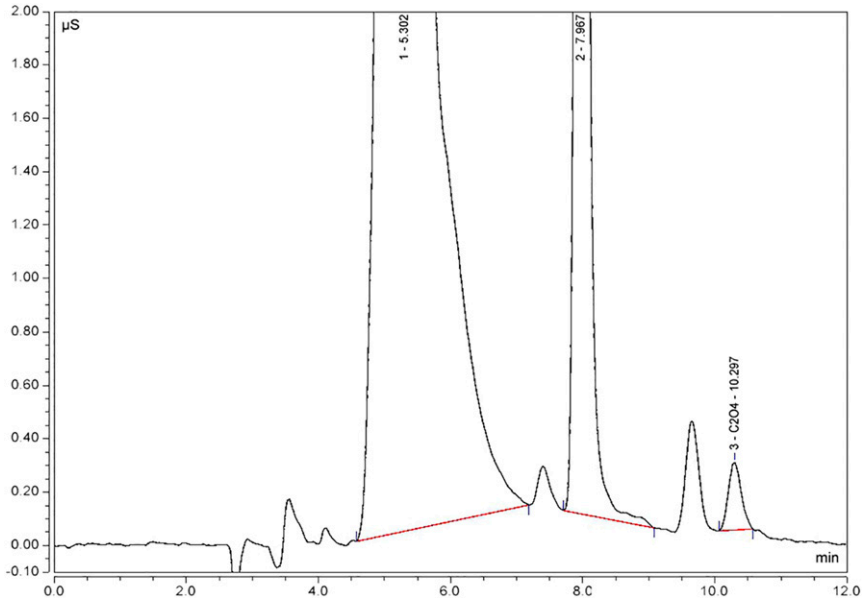

Fig. 5. IC of residues from Funnel 1, showing the presence of oxalate.

Hao Zhao for assisting in the collection of residue samples; Ganrong Wang and Lijing Zheng for providing help in the ion chromatography analysis; and two reviewers for their constructive comments. This research was supported by the Min Kwaan Chinese Archaeology Fund from the Stanford Archaeology Center, a summer research grant from Center for East Asian Studies, a travel grant from Stanford Archaeology Center, and a private donor.

1. Wen S, Yuan T (1983) *Yinxu Buci Yanjiu: Kexue Jishu Pian (A Study of Oracle Bones from Yinxu: Science and Technology)* (Sichuansheng Shehui Kexueyuan, Chengdu, China), 1st Ed.
2. Zhang D (1994) Yinshang jiuwenhua chulun (A preliminary study of Shang alcohol culture). *Zhongyuan Wenwu* 3:19–24.
3. Chen M (1956) *Yinxu Buci Zongshu (A Comprehensive Study of the Oracle Bone Inscriptions from Yinxu)* (Kexue, Beijing).
4. Huang HT (2000) *Science and Civilisation in China. Vol 6: Biology and Biological Technology. Part V: Fermentations and Food Science.* (Cambridge Univ Press, Cambridge, UK).
5. Li Y (1962) Dui woguo niangjiu qiyuan de tantao (The origin of alcoholic beverages in China). *Kaogu* 1:41–44.
6. Bao Q, Zhou J (2007) *Zhongguo Chuantong Gongyi Quanji: Niangzao (Chinese Traditional Technology: Brewing)* (Daxiang, Zhengzhou, China), 1st Ed.
7. McGovern PE, et al. (2004) Fermented beverages of pre- and proto-historic China. *Proc Natl Acad Sci USA* 101(51):17593–17598.
8. Shaanxi Provincial Institute of Archaeology (2012) *Xi'an Mijiaya–Xinshiqi Shidai Yizhi 2004-2006 Kaogu Fajue Baogao (2004–2006 Excavation Report of the Neolithic Site Mijiaya in Xi'an)* (Kexue, Beijing).
9. Institute of Archaeology, Chinese Academy of Social Sciences (1991) *Zhongguo Kaoguxue Zhong Tanshisi Niandai Shujuji (Radiocarbon Dates in Chinese Archaeology 1965–1991)* (Cultural Relics Publishing House, Beijing).
10. Yang Y (2013) *Shaanxi Yangguanzhai Yizhi Yangshao Wenhua Zhongwanqi Qihou Huanjing Jilu Ji Yizhi Gurenlei Dui Quyu Huanjin Yicun (The Climatic Record and Human-environmental Relations from Middle to Late Yangshao Period: A Case Study at Yangguanzhai, Shaanxi).* Master's thesis (Xibei University, Xi'an, China).
11. Piperno DR (2006) *Phytoliths: A Comprehensive Guide for Archaeologists and Paleoecologists* (AltaMira Press, Lanham, MD).
12. Ball T, Gardner JS, Brotherson JD (1996) Identifying phytoliths produced by the inflorescence bracts of three species of wheat (*Triticum monococcum* L.,*T. dicoccon* Schrank., and *T. aestivum* L.) using computer-assisted image and statistical analyses. *J Archaeol Sci* 23(4):619–632.
13. Ball TB, Gardner JS, Anderson N (1999) Identifying inflorescence phytoliths from selected species of wheat (*Triticum monococcum*, *T. dicoccon*, *T. dicoccoides*, and *T. aestivum*) and barley (*Hordeum vulgare* and *H. spontaneum*) (Gramineae). *Am J Bot* 86(11):1615–1623.
14. Ball TB, Ehlers R, Standing MD (2009) Review of typologic and morphometric analysis of phytoliths produced by wheat and barley. *Breed Sci Jpn* 59(4):55–102.
15. Lu H, et al. (2009) Phytoliths analysis for the discrimination of Foxtail millet (*Setaria italica*) and Common millet (*Panicum miliaceum*). *PLoS One* 4(2):e4448.
16. Weisskopf AR, Lee G-A (2014) Phytolith identification criteria for foxtail and broomcorn millets: A new approach to calculating crop ratios. *Archaeol Anthropol Sci* 8(1):29–42.
17. Liu L, Ma S, Cui J (2014) Identification of starch granules using a two-step identification method. *J Archaeol Sci* 52:421–427.
18. Ball TB, et al. (December 2015) A morphometric study of variance in articulated dendritic phytolith wave lobes within selected species of Triticeae and Aveneae. *Veg Hist Archaeobotany*, 10.1007/s00334-015-0551-x.
19. Samuel D (1996) Investigation of Ancient Egyptian baking and brewing methods by correlative microscopy. *Science* 273(5274):488–490.
20. Dronzek BL, Hwang P, Bushuk W (1972) Scanning electron microscopy of starch from sprouted wheat. *Cereal Chem* 49:232–239.
21. Sun Z, Henson CA (1990) Degradation of native starch granules by barley α-glucosidases. *Plant Physiol* 94(1):320–327.
22. Henry AG, Hudson HF, Piperno DR (2009) Changes in starch grain morphologies from cooking. *J Archaeol Sci* 36(3):915–922.
23. Briggs DE, Brookes PA, Stevens R, Boulton CA (2004) *Brewing: Science and Practice* (Taylor & Francis, London).
24. McGovern PE (2009) *Uncorking the Past: The Quest for Wine, Beer, and Other Alcoholic Beverages* (Univ of California Press, Berkeley).
25. Michel RH, McGovern PE, Badler VR (1992) Chemical evidence for ancient beer. *Nature* 360(6399):24.
26. Michel RH, McGovern PE, Badler VR (1993) The first wine and beer: Chemical detection of ancient fermented beverages. *Anal Chem* 65(8):408A–413A.
27. McGovern PE, et al. (2005) Chemical identification and cultural implications of a mixed fermented beverage from Late Prehistoric China. *Asian Perspect* 44(2):249–275.
28. Delcour JA, Hoseney RC (2010) *Principles of Cereal Science and Technology* (American Association of Cereal Chemists International, St. Paul, MN).
29. Boivin N, Fuller DQ, Crowther A (2012) Old World globalization and the Columbian exchange: Comparison and contrast. *World Archaeol* 44(3):452–469.
30. Jones M, et al. (2011) Food globalization in prehistory. *World Archaeol* 43(4):665–675.
31. Chen FH, et al. (2015) Agriculture facilitated permanent human occupation of the Tibetan Plateau after 3600 B.P. *Science* 347(6219):248–250.
32. Flad R, Li S, Wu X, Zhao Z (2010) Early wheat in China: Results from new studies at Donghuishan in the Hexi Corridor. *Holocene* 20(6):955–965.
33. Yu Y (1997) Han. *Food in Chinese Culture: Anthropological and Historical Perspectives*, ed Chang KC (SMC Publishing, Taipei, Taiwan), pp 53–83.
34. Liu L (2007) *The Chinese Neolithic: Trajectories to Early States* (Cambridge Univ Press, Cambridge, UK).
35. Jennings J, Bowser BJ (2009) Drink, power and society in the Andes: An introduction. *Drink, Power, and Society in the Andes*, eds Jennings J, Bowser BJ (Univ Press of Florida, Gainesville), pp 1–27.
36. Liang X (1987) Shilun Shaanxi Miaodegou II culture (A Discussion on Shaanxi Miaodigou II Culture). *Kaogu Xuebao* 04:397–412.
37. Liang X (1994) Shilun keshengzhuang Erqi wenhua (A discussion on the Keshengzhuang Culture). *Kaogu Xuebao* 04:397–424.
38. An C, Feng Z, Tang L (2004) Environmental change and cultural response between 8000 and 4000 cal. yr BP in the western Loess Plateau, northwest China. *J Quat Sci* 19(6):529–535.
39. GPICRA (Gansu Provincial Institute of Cultural Relics and Archaeology) (2006) *Gansu Qin'an Dadiwan Xinshiqi Shidai Yizhi Fajue Baogao (Qin'an Dadiwan Excavation Report)* (Cultural Relics Publishing House, Beijing).

Supporting Information

Wang et al. 10.1073/pnas.1601465113

SI Text

Further Details of the Mijiaya Site. The Mijiaya site was discovered in 1923 by J. G. Anderson and excavated from 2004 to 2006. The excavations revealed three separate cultural strata belonging to established chronology in the region based on ceramic typology with associated radiocarbon dates: the Banpo IV phase (belonging to the late Yangshao period, 3400–2900 BC), the Miaodigou II phase (2800–2450 B.C) (36), and the Keshengzhuang phase (2400–2000 BC) (37). The entire site measures around 45 ha with cultural deposits 1.5–4 m in depth. A total of 166 Banpo IV pits were found, and the majority of them are regular in shape with flat bottoms, suggesting their initial function as storage pits (8). The ceramic artifacts from the earliest stratum are Banpo IV styles that are comparable to the related sites in the region, including Xiehu in Lantian, Xijing in Shanxian, and Quanhucun in Huaxian. Pollen analysis indicates that the climate of the Wei River valley was semiarid during the Banpo IV phase, characterized by steppe vegetation and herbaceous plants dominating the pollen assemblage (38).

Social Complexity During the Late Yangshao Period. The settlement pattern of the late Yangshao period is characterized by site nucleation and a two- or three-tiered settlement hierarchy. Several large regional centers emerged along the Wei River valley for the first time, including Dadiwan (100 ha) and Gaositou in Gansu and Anban (70 ha) in Shaanxi. Palace-like architectures are present in all three sites, occupying the central locations of the settlements. At Dadiwan, for example, a multiroomed structure (F901; 290 m^2 in size) was found in the center of the site (39). Ceramic remains found in the structure include large-sized pottery storage urns, pile-up bowls, and vessels of regularly graduated sizes. A large hearth was located in the center of the major room. The house may have functioned as a central place for activities of regional communities. Compared with the sites in the middle Yangshao period, public buildings in the late Yangshao period became bigger in size, and they are likely to have served for ritual ceremonies and feasting, at both local and regional levels (34). The construction of large public buildings during the late Yangshao period implies an increased level of social hierarchy and complexity. Competitive feasting is likely to have been conducted by the regional elite for obtaining high social status.

SI Materials and Methods

Field Sampling. The field sampling took place in the Jingwei Archaeological Station in Xi'an, China. All artifacts for this study were curated in storage. Only new and sterile plastic bags, test tubes, pipettes, toothbrushes, and razor blades were used during the sampling process. The procedure used is as follows.

First, three residue samples for IC analysis were taken from the interior surfaces of Funnel 1, Pot 3, and Pot 5. The residues were yellowish in color and firmly adhering to the interior vessel walls. Residues from each vessel were scrapped off by using a clean razor blade. By using the same method, two control samples were obtained from the soil adhering to the exterior surface of Pot 5 (one for IC and one for microbotanical analysis), and one control sample was taken from the conservation plaster material on the interior surface of Funnel 2.

Second, all artifacts were subjected to sonication. An ultrasound bath was used to extract residues from Funnel 1, Funnel 2, Pot 1, and a control sample (stone adze). Each artifact was placed in a new, polyvinyl bag with ~15 mL of distilled water. For Funnel 1, Funnel 2, and Pot 1, only the mouth part (up to 2.5–3 cm from the opening) was immersed in the distilled water. For the stone adze, the entire artifact was immersed. The bag containing the artifact then was placed into the bath for 3 min. After 3 min, the artifact was removed from the bag. For artifacts that were too big to be placed in the ultrasound bath (Pot 2, Pot 3, Pot 4, Pot 5, Pot 6, Pot7), ultrasonic toothbrushes were used. First, each artifact was placed in a new polyvinyl bag. The interior surface of the artifact was then brushed gently with an ultrasonic toothbrush and at the same time a pipette was used to add distilled water to rinse the surface. Only a new ultrasonic toothbrush and a new pipette were used for each artifact. The water and all sediment from the bag were transferred into a new 15-mL test tube. Each tube was stored in a sealed plastic bag before laboratory analysis.

Laboratory Techniques for Starch and Phytolith Analyses. The protocol for starch and phytolith extraction is as follows:

Sample concentration. Each 15-mL tube containing sediment and water was topped off with distilled water and placed in a centrifuge (Eppendorf 5804, Hamburg, Germany) for 5 min at 1,500 rpm to concentrate the sample at the bottom of the tube. The supernatant was then decanted.

Dispersion. Four microliters of 0.1% EDTA ($Na_2EDTA{\bullet}2H_2O$) solution was added to each tube. Then the capped tubes were placed in an automatic shaker for 2 h to disperse the sediments. After being removed from the shaker, the tubes were filled to 15 mL with distilled water and centrifuged for 5 min at 1,500 rpm, and the supernatant was decanted.

Heavy liquid separation. Four microliters of heavy liquid sodium polytungstate at a specific gravity of 2.35 was added to the tubes. The tubes were then centrifuged for 15 min at 1,000 rpm. The top 1- to 2-mm layer of organics was carefully removed from each test tube by a new pipette and then transferred into a new 15-mL tube. The samples were topped off with distilled water and centrifuged for 5 min at 1,500 rpm to concentrate the starch and phytolith at the bottom of the tube, and the supernatant was decanted. The rinse was repeated two more times to remove any remaining sodium polytungstate.

Slide mounts and microscope scanning. An aliquot of residue sample was extracted with a pipette to a microscope slide and allowed to dry. Then the residue was resuspended in 30–40 μL of 50% (vol/vol) glycerol and 50% (vol/vol) distilled water. A coverslip was placed on top, and the edges were sealed with nail polish. All slides were scanned under a Zeiss Axio Scope A1 fitted with polarizing filters and DIC optics, at 200× and 400× for both starch and phytoliths.

Beer-Brewing Experiments. The brewing experiments were based on four sets of cereal grains. The four experimental sets consisted of broomcorn millet (40 g), foxtail millet (40 g), a mixture of broomcorn millet (30 g) and barley (10 g), and a mixture of foxtail millet (30 g) and barley (10 g), respectively. Each set went through three brewing steps, including malting, mashing and fermentation. The procedure is as follows:

First, grains were immersed in water until they began to germinate. The room temperature was around 20–28 °C. Most grains germinated after 8 d, and they were drained and dried. Next, the malted grains were crushed and mixed with heated water to achieve a final temperature of 65 °C. The temperature was maintained for 2 h. Finally, the mash was cooled in room temperature and allowed to ferment in a brewing container for 2 d. During fermentation each container was covered with a lid to create an anaerobic condition.

To obtain reference starch samples to compare with the ancient starches, we took starch samples during the experiment. Two to three malted seeds of broomcorn millet, foxtail millet, and barley were taken for microscopic observation, and two patterns were observed. First, all three types of malted grains had starches that

showed pittings, channelings, or fissures radiating from their centers. The centers of the grains appeared hollowed but the outer edges appeared undamaged (Fig. S3 *A*–*C*). Second, this type of damage was common and appeared in around 90% of broomcorn millet and foxtail millet starches; it was rare and appeared in about 1% of barley starches. A second batch of starch samples was taken from each set when mashing was done. Various levels of swelling and distortion were present in ∼5% of broomcorn millet, and 10–15% of the other three samples (Fig. S3 *D*, *G*, *J*, and *M*). When fermentation was finished, a third batch of starch samples was taken from each set. Three patterns were observed from all four brewing sets. First, pitted starch grains were still present, and their outer edges also appeared damaged (see arrows in Fig. S3 *E*, *H*, and *K*). Second, abundant starch grains exhibited swelling, distortion, and loss of extinction cross. Many starch grains merged into one another completely (Fig. S3 *F* and *O*). Compared with mashed samples, the fermented starch grains exhibited a higher level of swelling and distortion; extinction cross was not observed in many large starches. Third, some small-sized starch grains remained intact (see arrow in Fig. S3*L*). However, we were unable to produce quantified data from the fermented samples because a high proportion of the starch grains was gelatinized and merged together.

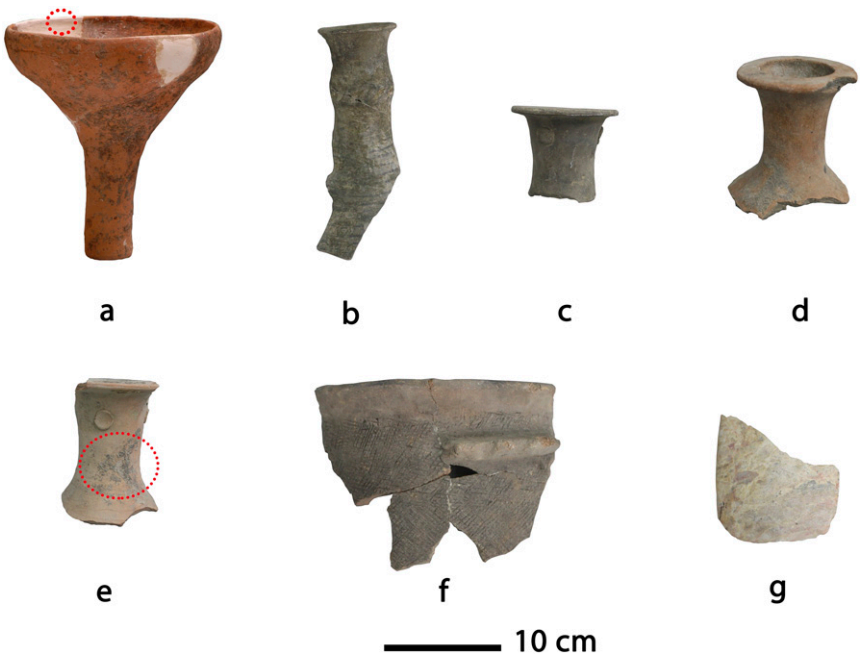

Fig. S1. Analyzed Mijiaya artifacts not included in Fig. 1. Artifacts and their discovery contexts from the upper row to the lower row: (*A*) funnel 2 (H78), red circle indicating the sampling location of control sample 3; (*B*) pot 1 (H82); (*C*) pot 2 (H82); (*D*) pot 4 (H82); (*E*) pot 5 (H78), red circle indicating the sampling location of control sample 1 and control sample 4; (*F*) pot 7 (H78); (*G*) stone adze (H78).

Fig. S2. Residues from the interior surface of funnel 1.

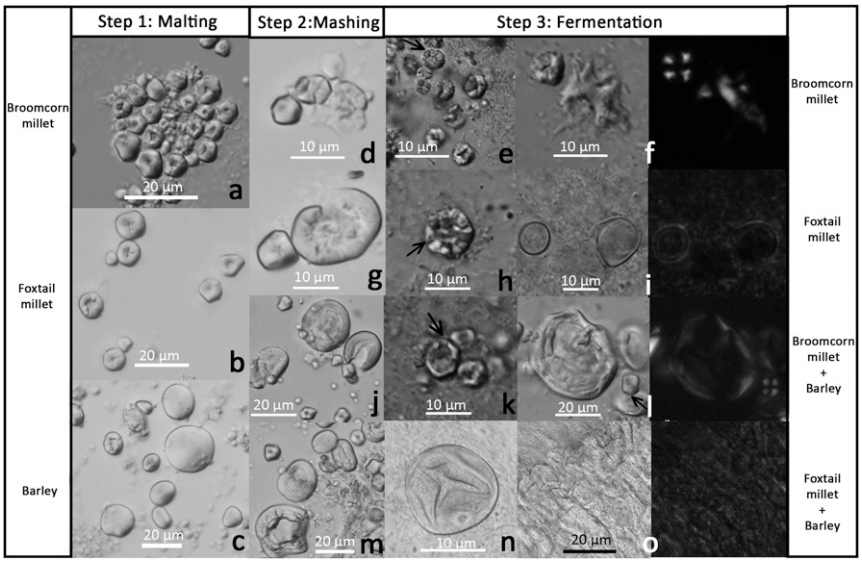

Fig. S3. Starch grains from brewing experiments: (*A*) Malted broomcorn millet (*P. miliaceum*); (*B*) malted foxtail millet (*S. italica*); (*C*) malted barley (*H. vulgare*); (*D*) mashed broomcorn millet; (*E*) fermented broomcorn millet, showing pittings and damaged outer edges; (*F*) fermented broomcorn millet, showing pitting (*Left*) and gelatinization (*Right*); (*G*) mashed foxtail millet; (*H*) fermented foxtail millet, showing pitting and damaged outer edge; (*I*) fermented foxtail millet, showing gelatinization, merging, and loss of extinction cross; (*J*) mashed broomcorn millet and barley; (*K*) fermented broomcorn millet and barley, showing big hollows in the centers and damaged outer edges; (*L*) fermented broomcorn millet and barley, showing one gelatinized grain (*Left*) and one undamaged grain (*Right*); (*M*) mashed foxtail millet and barley; (*N*) a starch grain from fermented foxtail millet and barley, showing channeling and distortion; (*O*) a cluster of completely merged starch grains and loss of extinction cross from fermented foxtail millet and barley.

Table S1. Morphology of starch grains

ID	Grain shape	Size range (mean), μm	Hilum	Fissures	Lamellae	Extinction cross
Broomcorn millet, *P. miliaceum*	Polygonal and subround, facetted	3.77–13.87 (9.06)	Mostly centric	"Y", "V", or linear forms	Absent	"+" Shape with straight arms
Triticeae	Round or oval, flat surface	6.85–38.38(21.30)	Centric	Rare	Visible on large grains	Mostly "+" shape
Job's tears, *C. lacryma-jobi*	Polygonal and subround, facetted	5.1–28.28(16.3)	Centric or eccentric	Common, "Y", "V", and linear forms, or many fine lines radiating to the edge	Visible on some	Mostly straight, sometimes with bent or Z-shaped arms
Snake gourd root, *T. kirilowii*	Spherical or regular oval, bell-shape, semispherical, and nearly semispherical with facets	8.61–30.61(18.85)	Centric or eccentric	Some with short linear fissure	Visible on large grains	Mostly with bent arms, sometimes straight
Yam, *Dioscorea* sp.	Irregular triangular or oval shape	12.34–23.11(18.09)	Eccentric	Some with short linear fissure	Visible on most grains	Bent arms
Lily, *Lilium* sp.	Irregular triangular	16.88–34.71(24.41)	Eccentric	Some with short linear fissure	Visible on most grains	Bent arms

Table S2. Description of phytolith morphometries analyzed

Name	Description
Form factor	Equals 4 × Area × π/Perimeter, it is 1.0 for a perfect circle and diminishes for irregular shapes.
Roundness	Equals 4 × Area/π × Length^2, it is 1.0 for perfect circle and diminishes with elongation of the feature.
Solidity	Ratio of area to convex area; It is 1.0 for a perfectly convex shape, diminishes if there are surface indentations.
Compactness	Ratio of the equivalent diameter to the length.
Convexity	Ratio of convex perimeter to perimeter; It is 1.0 for a perfectly convex shape, diminishes if there are surface indentations.
Aspect ratio	Equals length/width.

Table S3. Range of mean morphometries of articulated dendritic wave lobes observed in all bract types from all inflorescence locations for all accessions of selected species from modern comparative species: *Triticum*, *Avena*, *Secale*, *Agropyron*, and *Bromus*

Genus	*Triticum*					*Avena*	*Secale*	*Agropyron*		*Bromus*
Species	*T. aestivum*	*T. dicoccoides*	*T. dicoccon*	*T. durum*	*T. monococcum*	*A. sativa*	*S. cereale*	*A. cristatum*	*A. mongolicum*	*B. japonica*
Form factor	0.607–0.725	0.646–0.711	0.643–0.745	0.623–0.707	0.668–0.817	0.635–0.721	0.635–0.709	0.691–0.744	0.672–0.711	0.680–0.739
Roundness	0.500–0.614	0.517–0.608	0.531–0.619	0.552–0.603	0.532–0.617	0.526–0.616	0.504–0.626	0.526–0.603	0.512–0.594	0.537–0.614
Solidity	0.936–0.973	0.940–0.970	0.918–0.979	0.922–0.957	0.954–0.984	0.904–0.978	0.928–0.968	0.966–0.979	0.952–0.972	0.963–0.974
Compactness	0.691–0.781	0.714–0.777	0.724–0.785	0.738–0.769	0.725–0.783	0.718–0.783	0.706–0.774	0.738–0.774	0.712–0.769	0.730–0.782
Convexity	0.921–0.944	0.912–0.941	0.905–0.948	0.889–0.940	0.935–0.949	0.907–0.946	0.922–0.942	0.937–0.948	0.937–0.944	0.941–0.947
Aspect ratio	1.463–1.638	1.469–1.710	1.500–1.667	1.463–1.611	1.490–1.710	1.423–1.775	1.503–1.690	1.482–1.826	1.458–1.758	1.435–1.641

Table S4. Range of mean morphometries of articulated dendritic wave lobes observed in all bract types from all inflorescence locations for all accessions of selected species from modern comparative species: *Elytrigia*, *Leymus*, *Roegneria*, *Hordeum*

Genus	*Elytrigia*	*Leymus*	*Roegneria*			*Hordeum*				
Species	*E. elongata*	*L. secalinus*	*R. mayebarana*	*R. ciliaris*	*R. pendulina*	*H. vulgare*	*H. bulbosum*	*H. comosum*	*H. secalinum*	*H. distichon*
Form factor	0.719–0.742	0.706–0.740	0.705–0.741	0.719–0.737	0.621–0.746	0.644–0.736	0.708–0.757	0.717–0.744	0.693–0.760	0.642–0.748
Roundness	0.582–0.628	0.573–0.625	0.552–0.603	0.588–0.613	0.621–0.629	0.448–0.617	0.563–0.632	0.564–0.634	0.525–0.644	0.458–0.626
Solidity	0.965–0.983	0.960–0.973	0.967–0.978	0.972–0.980	0.969–0.976	0.954–0.981	0.977–0.988	0.971–0.977	0.978–0.983	0.979–0.985
Compactness	0.760–0.791	0.754–0.789	0.741–0.774	0.765–0.782	0.786–0.792	0.664–0.784	0.748–0.794	0.748–0.796	0.721–0.802	0.671–0.790
Convexity	0.941–0.948	0.939–0.946	0.943–0.949	0.942–0.947	0.945–0.946	0.934–0.952	0.943–0.950	0.943–0.945	0.945–0.950	0.945–0.948
Aspect ratio	1.412–1.580	1.392–1.562	1.489–1.641	1.463–1.544	1.414–1.449	1.497–2.090	1.458–1.657	1.449–1.707	1.410–1.829	1.482–2.123

Table S5. Mean morphometries of articulated dendritic wave lobes observed in Mijiaya residue samples

	Sample				
Morphometry	Funnel 1	Pot 2	Pot 3	Pot 4	Pot 5
ND	2	52	24	10	27
NL	33	307	131	97	208
Form factor	0.729788	0.696355	0.668985	0.657271	0.715702
Roundness	0.547273	0.488202	0.455939	0.474625	0.533909
Convexity	0.949152	0.948322	0.947763	0.935229	0.942255
Solidity	0.980485	0.971811	0.971519	0.95774	0.975072
Compactness	0.736576	0.693264	0.669	0.684094	0.726654
Aspect ratio	1.666182	1.948433	2.07529	2.03824	1.737486

ND, the number of articulated dendritics that formed the wave lobes measured; NL, the number of wave lobes measured in each sample.

Table S6. Comparison of mean morphometries of articulated dendritic waves in Mijiaya vessels with the range of mean wave morphometries from selected species from modern comparative species

Reference taxon	Sample	Funnel 1	Pot 2	Pot 3	Pot 4	Pot 5
	ND	2	52	24	10	27
	NL	33	307	131	97	208
Triticum aestivum	Form factor		x	x	x	x
	Roundness	x				x
	Solidity		x	x	x	
	Compactness	x	x			x
	Convexity				x	x
	Aspect ratio					
Triticum dicoccoides	Form factor	x	x	x	x	
	Roundness	x				x
	Solidity				x	
	Compactness	x				x
	Convexity				x	
	Aspect ratio	x				
Triticum dicoccon	Form factor	x	x	x	x	x
	Roundness	x				x
	Solidity		x	x	x	x
	Compactness	x				x
	Convexity		x	x	x	x
	Aspect ratio	x				
Triticum durum	Form factor		x	x	x	
	Roundness					
	Solidity					
	Compactness					
	Convexity				x	
	Aspect ratio					
Triticum monococcum	Form factor	x	x	x		x
	Roundness	x				x
	Solidity	x	x	x	x	x
	Compactness	x				x
	Convexity	x	x	x	x	x
	Aspect ratio	x				
Avena sativa	Form factor		x	x	x	x
	Roundness	x				x
	Solidity		x	x	x	x
	Compactness	x				x
	Convexity				x	x
	Aspect ratio	x				x
Secale cereale	Form factor		x	x	x	
	Roundness	x				x
	Solidity				x	
	Compactness	x				x
	Convexity				x	x
	Aspect ratio	x				
Agropyron cristatum	Form factor	x	x			x
	Roundness	x				x
	Solidity		x	x		x
	Compactness					
	Convexity		x	x		x
	Aspect ratio	x				x
Agropyron mongolicum	Form factor		x			
	Roundness	x				x
	Solidity		x	x	x	
	Compactness	x				x
	Convexity					x
	Aspect ratio	x				x
Elytrigia elongata	Form factor	x				
	Roundness					
	Solidity	x	x	x		x
	Compactness					
	Convexity		x	x		x
	Aspect ratio					

Table S6. Cont.

Reference taxon	Sample	Funnel 1	Pot 2	Pot 3	Pot 4	Pot 5
Leymus secalinus	Form factor	x				x
	Roundness					
	Solidity		x	x		
	Compactness					
	Convexity					x
	Aspect ratio					
Roegneria mayebarana	Form factor	x				x
	Roundness					
	Solidity		x	x		x
	Compactness					
	Convexity	x	x	x		
	Aspect ratio					
Roegneria ciliaris	Form factor	x				
	Roundness					
	Solidity	x				x
	Compactness					
	Convexity					x
	Aspect ratio					
Roegneria pendulina	Form factor	x	x	x	x	x
	Roundness					
	Solidity		x	x		x
	Compactness					
	Convexity					
	Aspect ratio					
	Elongation					
Bromus japonica	Form factor	x	x			x
	Roundness	x				
	Solidity		x	x		
	Compactness	x				
	Convexity					x
	Aspect ratio					
Hordeum vulgare	Form factor	x	x	x	x	x
	Roundness	x	x	x	x	x
	Solidity	x	x	x	x	x
	Compactness	x	x	x	x	x
	Convexity	x	x	x	x	x
	Aspect ratio	x	x	x	x	x
Hordeum bulbosum	Form factor	x				x
	Roundness					
	Solidity	x				
	Compactness					
	Convexity	x	x	x		
	Aspect ratio					
Hordeum comosum	Form factor	x				
	Roundness					
	Solidity		x	x		x
	Compactness					
	Convexity					
	Aspect ratio	x				
Hordeum secalinum	Form factor	x	x			x
	Roundness	x				x
	Solidity	x				
	Compactness	x				x
	Convexity	x	x	x		
	Aspect ratio	x				x
Hordeum distichon	Form factor	x	x	x	x	x
	Roundness	x	x		x	x
	Solidity	x				
	Compactness	x	x		x	x
	Convexity		x	x		
	Aspect ratio	x	x	x	x	x

ND, the number of articulated dendritics that formed the wave lobes measured; NL, the number of wave lobes measured in each sample; x, mean for the sample falls within the range of means for the reference taxon.